RUB-TPII-04/2013

Theoretical description and measurement of the pion-photon transition form factor*

S. V. Mikhailov†

Bogoliubov Laboratory of Theoretical Physics,

JINR, 141980 Dubna, Russia

A. V. Pimikov‡

Departamento de Física Teórica -IFIC,

Universidad de Valencia-CSIC,

E-46100 Burjassot (Valencia), Spain

Bogoliubov Laboratory of Theoretical Physics,

JINR, 141980 Dubna, Russia

N. G. Stefanis§

Institut für Theoretische Physik II,

Ruhr-Universität Bochum,

D-44780 Bochum, Germany

arXiv:1401.4303v2 [hep-ph] 28 Feb 2014

Abstract

Detailed predictions for the scaled pion-photon transition form factor are given, derived with the method of light-cone sum rules and using pion distribution amplitudes with two and three Gegenbauer coefficients obtained from QCD sum rules with nonlocal condensates. These predictions agree well with all experimental data that are compatible with QCD scaling (and collinear factorization), but disagree with the high-Q^2 data of the BaBar Collaboration that grow with the momentum. A good agreement of our predictions with results obtained from AdS/QCD models and Dyson-Schwinger computations is found.

PACS numbers: 12.38.Lg, 12.38.Bx, 13.40.Gp, 11.10.Hi

*Dedicated to the memory of our beloved friend and collaborator Alexander P. Bakulev.

†Electronic address: mikhs@theor.jinr.ru

‡Electronic address: pimikov@theor.jinr.ru

§Electronic address: stefanis@tp2.ruhr-uni-bochum.de

I. INTRODUCTION

The pion-photon transition form factor for two highly virtual photons, $F^{\gamma^*\gamma^*\pi^0}(q_1^2, q_2^2)$, is considered to be a key hard exclusive process because it emerges as a consequence of the factorization properties of quantum chromodynamics (QCD). All binding effects, governed by nonperturbative QCD interactions, are isolated within the pion distribution amplitudes $\varphi_\pi(x, \mu^2)$ (here μ^2 is the normalization scale of order 1 GeV^2) for finding valence partons in the pion carrying a longitudinal momentum fraction x (struck quark) and $\bar{x} \equiv 1 - x$ (spectator) [1, 2]. Assuming $q_1^2 = -Q^2 \gg q_2^2 = -q^2 > 0$, one can calculate $F^{\gamma^*\gamma^*\pi^0}(Q^2, q^2)$ in QCD perturbation theory including evolution [1, 3].

On the experimental side, the meson-photon transition form factors can be measured using two-photon events is so-called single-tag experiments of the generic form $e^+e^- \longrightarrow e^+e^-M$, where M is a pseudoscalar meson π^0, η, η', in which only one electron (positron) is tagged, whereas the untagged electron (positron) induces an uncertainty on the small virtuality $|q^2|$ of the quasi-real photon. However, such a photon has not a pointlike structure, rendering the direct application of perturbative QCD unreliable. Therefore, one has to employ another technique that allows one to approach the real-photon limit in a more prudent way. In our approach [4–9], this goal is achieved using the method of light-cone sum rules [10–12] — see next section. Our theoretical predictions, obtained this way, for the two-photon process $\gamma^* + \gamma \longrightarrow \pi^0(\eta, \eta')$ are compared with the experimental data of various collaborations [13–16] (pion case) and [14, 17] (η, η') in Sec. III. The main characteristic of our predictions for $Q^2 F^{\gamma^*\gamma\pi^0}(Q^2, q^2 \to 0)$ is a scaling behavior above about $Q^2 \simeq 10$ GeV^2, which is in accordance with the QCD asymptotic prediction [1], both in trend and magnitude. The auxetic [9] behavior of the BaBar data for this process in this region cannot be reproduced within collinear QCD.

II. THEORETICAL DESCRIPTION OF THE PION-PHOTON TRANSITION FORM FACTOR

The calculation of the pion-photon transition form factor

$$\int d^4z e^{-iq_1\cdot z} \langle \pi^0(P)|T(j_\mu(z) j_\nu(0))|0\rangle = i\epsilon_{\mu\nu\alpha\beta} q_1^\alpha q_2^\beta F^{\gamma^*\gamma^*\pi^0}(Q^2, q^2) \ , \tag{1}$$

where j_μ is the quark electromagnetic current, is based on the following light-cone sum rule [10, 12]

$$Q^2 F^{\gamma^*\gamma^*\pi}\left(Q^2,q^2\right) \;=\; \frac{\sqrt{2}}{3} f_\pi \left[\frac{Q^2}{m_\rho^2+q^2}\int_{x_0}^1 \exp\left(\frac{m_\rho^2 - Q^2\bar{x}/x}{M^2}\right)\bar{\rho}(Q^2,x)\frac{dx}{x} + \int_0^{x_0}\bar{\rho}(Q^2,x)\frac{Q^2 dx}{\bar{x}Q^2+xq^2}\right]. \tag{2}$$

Here, the integration limits are defined by $x_0 = Q^2/\left(Q^2+s_0\right)$ and $s = \bar{x}Q^2/x$, whereas M^2 is the Borel parameter and $m_\rho = 0.77$ GeV denotes the mass of the ρ meson[1]. The main ingredient in the above sum rule is the spectral density $\bar{\rho}(Q^2,x) = (Q^2+s)\rho^{\rm pert}(Q^2,s)$, where

$$\rho^{\rm pert}(Q^2,s) = \frac{1}{\pi}{\rm Im}F^{\gamma^*\gamma^*\pi^0}\left(Q^2,-s-i\varepsilon\right) = \rho_{\text{tw-2}} + \rho_{\text{tw-4}} + \rho_{\text{tw-6}}. \tag{3}$$

Each term corresponds to a definite twist contribution and is calculable with the help of the analogous term of the hard-scattering amplitude convoluted with the pion distribution amplitude of the same twist.

In our analysis, presented in this note, we restrict our considerations to the level of twist four, so that the transition form factor acquires the form

$$F_{\gamma^*\gamma^*\pi^0} \sim \left[T_{\rm LO} + a_s(\mu^2)T_{\rm NLO} + a_s^2(\mu^2)T_{\rm NNLO_{\beta_0}} + \ldots\right]\otimes\varphi_\pi^{(2)}(x,\mu^2) + \mathcal{O}\left(\frac{\delta^2}{Q^4}\right)\,, \tag{4}$$

where the pion distribution amplitude (DA) $\varphi_\pi^{(2)}$ of twist two represents the nonperturbative part of the factorized initial expression at the momentum scale $\mu^2 \approx 1$ GeV^2 and δ^2 sets the scale of the twist-four term. In our analysis we vary $\delta^2 = 0.19$ GeV^2, (estimated in [4]), in the range $[0.15 - 0.23]$ GeV^2, [5], and use for the twist-four pion DA its asymptotic form $\varphi_\pi^{(4)}(x,\mu^2))(80/3)\delta^2(\mu^2)x^2(1-x)^2$. The meson DA can be expressed in terms of the coefficients a_n as an expansion over Gegenbauer harmonics, viz., $(\xi = x - \bar{x})$

$$\varphi_\pi^{(2)}(x,\mu^2) = 6x\bar{x}\left(1 + \sum_{n=2,4,\ldots}^{\infty} a_n C_n^{3/2}(\xi)\right) \tag{5}$$

with the normalization $\int_0^1 dx\varphi_\pi^{(2)}(x,\mu^2) = 1$. To compare with the experimental data at higher values $Q^2 > \mu^2$, one has to take into account evolution effects. This is done here at the level of the next-to-leading-order (NLO) Efremov-Radyushkin-Brodsky-Lepage (ERBL) evolution equation [1, 19]. In the next section, we will present predictions based on the two Gegenbauer coefficients a_2 and a_4 determined long ago in [20] via the moments $\langle\xi^N\rangle_\pi \equiv \int_0^1 dx(2x-1)^N\varphi_\pi^{(2)}(x,\mu^2)$ with

[1] In the actual calculation we have also taken into account the width of the vector meson, as applied in [18]

the help of QCD sum rules and nonlocal condensates [21–23]. In addition, we will also show recent predictions [7, 9] derived in a 3D analysis that makes use of the next higher Gegenbauer coefficient a_6 that was found in [20] to be compatible with zero but with large uncertainties. The crucial characteristics of this type of distribution amplitudes is that their endpoints are strongly suppressed. This is related to the finite virtuality of the vacuum quarks $\lambda_q^2 = 0.40(5)$ GeV^2 which implies that quarks at distances of the order of $\Lambda \sim 1/\lambda \approx 0.31$ fm get correlated. As a result, vacuum quarks with vanishing virtuality cannot migrate into the pion bound state [24, 25], because this is protected by a mass gap.

III. COMPARING THEORY WITH EXPERIMENTAL DATA

The evaluation of the sum rule in Eq. (2) is performed with the following ingredients: (i) We include in the spectral density the NLO radiative corrections and also the twist four contribution. (ii) The contributions related to the β_0 part of the next-to-next-to-leading-order (NNLO) corrections [18] and the twist-six term, computed in [26, 27], are included in the form of systematic uncertainties. This is justified, because for the values of the Borel parameter we use around an average of $\overline{M^2} = 0.75$ GeV^2, both mentioned contributions are small, but enter with opposite signs so that they partially cancel each other. (Note that using a larger value $M^2 = 1.5$ GeV^2 as in [26], the twist-six term becomes negligible.) (iii) The evolution is taken into account at the NLO using the default scale setting $\mu_{\rm R}^2 = \mu_{\rm F}^2 = Q^2$ and using the values $\Lambda_{\rm QCD}^{(3)} = 370$ MeV and $\Lambda_{\rm QCD}^{(4)} = 304$ MeV, consistent with $\alpha_s(M_Z^2) = 0.118$.

In Fig. 1, we present the results of our analysis for the pion DAs, extracted from the experimental data, graphing them in terms of the Gegenbauer coefficients a_n in Eq. (5). These coefficients, in both panels, have been obtained from the statistical analysis of two data sets: CELLO&CLEO&Belle (large left ellipsoid with the center named CCBe) and CELLO&CLEO&BaBar (small ellipsoid with the center named CCBa). The left panel of this figure shows the 3D confidence regions of the coefficients (a_2, a_4, a_6) as a continuous stack of rectangles, while the right panel reproduces a 2D slice of this 3D illustration. The vertices of the triangle on the left panel are located at the two best fit points, CCBe and CCBa, determined in the 3D analysis of the corresponding data sets, while the third point ✖ in the plane (a_2, a_4) denotes the BMS pion DA, derived from QCD sum rules with nonlocal condensates in [20]. Thus, the single (cut) plane shown on the right panel illustrates the results of the statistical analysis of the data from the viewpoint of the theoretical predictions. In this figure we use the χ^2-square

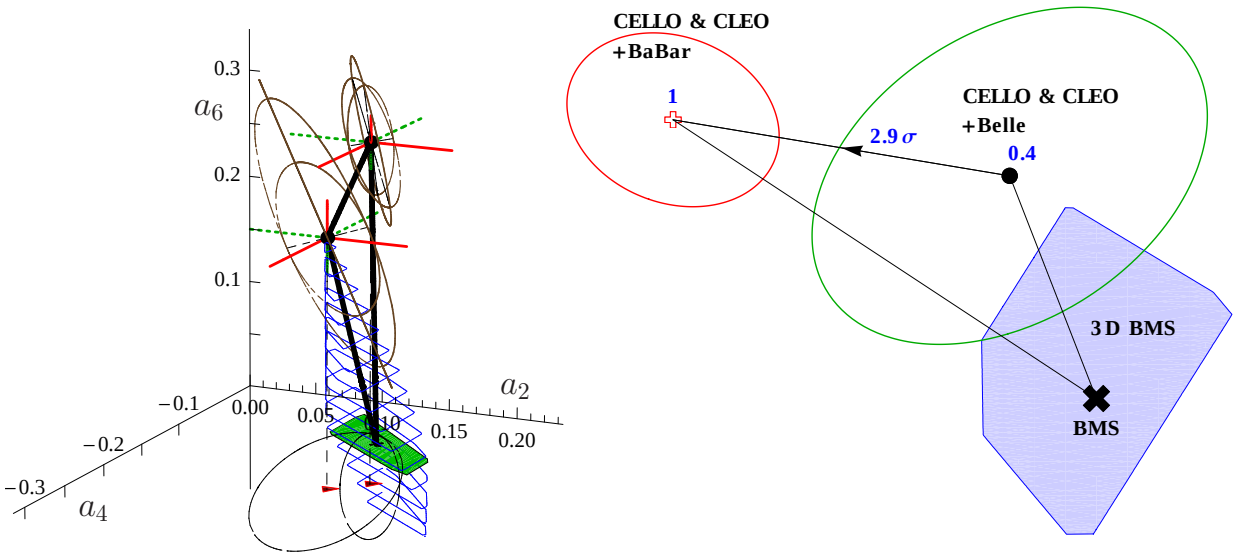

FIG. 1: **Left panel:** The 3D confidence regions for the Gegenbauer coefficients (a_2, a_4, a_6) extracted from the analysis of two data sets: CELLO&CLEO&Belle (large left ellipsoid represented by its main ellipses) and CELLO&CLEO&BaBar (small ellipsoid) in comparison with the QCD SR result shown as a series of (blue) "stairs" along the a_6 axis. The shaded (green) rectangle, next to the projections of the 3D ellipsoids, denotes the range of values of a_2 and a_4 determined by BMS via QCD sum rules with nonlocal condensates. The central points of the three 3D regions (large and small ellipsoids and BMS rectangle) build the vertices of a triangle. This triangle is also shown on the right panel of this figure. **Right panel:** Quantification of the disagreement between the two data sets, termed (CELLO & CLEO + Belle) vs. (CELLO & CLEO +BaBar) in comparison with the BMS region of (a_2, a_4) values (shaded blue area). The 2D slice of the 3D figure, presented on the left, is shown in terms of a triangle with the values of the χ^2-squared goodness of fit criterion χ^2/ndf marking its vertices.

goodness of fit criterion χ^2/ndf (with ndf = number of degrees of freedom) to mark the vertices of the triangle (right panel), CCBa – χ^2/ndf $\gtrsim 1$ and CCBe – χ^2/ndf ≈ 0.4. We indicate the level of disagreement between the two considered data sets quantitatively by means of the one standard deviation from the CELLO&CLEO&Belle best-fit point that reaches for the CCBa point the value $2.9\sigma_{\rm CCBe}$ (more technical details can be found in [9]). As one sees from this figure, a considerable part of the 3D BMS region — blue rectangle on the right panel — overlaps with the $1\sigma_{\rm CCBe}$ region of the CELLO&CLEO&Belle data.

Let us now compare the ingredients of our analysis and its predictions with other recent theoretical approaches. This comparison will be selective. Some examples of approaches (among many others) that can reproduce the growing trend of the BaBar data can be found in [30–34], while

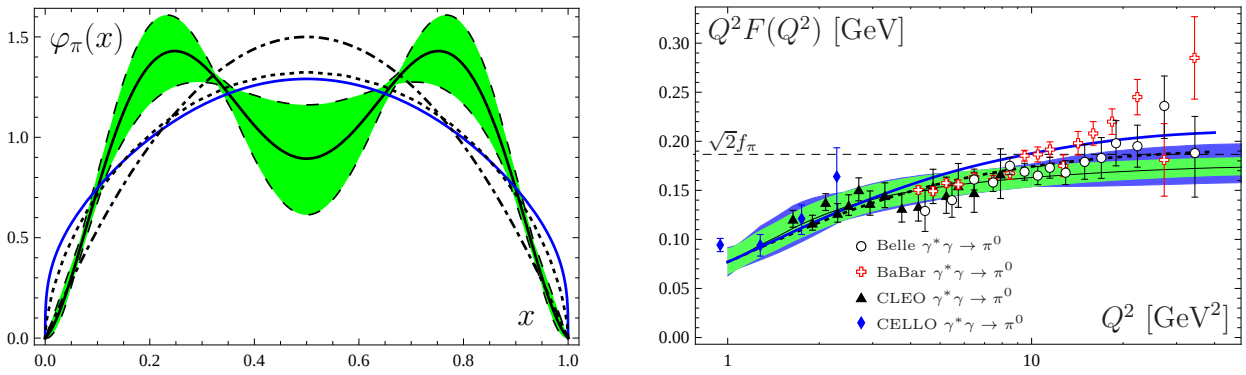

FIG. 2: **Left panel**: Profiles of various pion DAs at the normalization scale 2 GeV. The shaded band shows the "bunch" of the BMS DAs from [20], with the solid line inside denoting the BMS model DA. The dotted line is the model obtained in [28] from AdS/QCD, whereas the (blue) solid line represents the result derived in [29] using an approach based on the Dyson-Schwinger equation. For the sake of comparison, the asymptotic DA is also displayed — dashed-dotted line. **Right panel**: Predictions for the scaled pion-photon transition form factor in the momentum range covered by several experiments. The inner shaded band (in green) graphs our results for the BMS "bunch" shown on the left panel. The upper and lower narrower strips (in blue color) denote the additional areas of values emerging from the inclusion of the coefficient a_6 — 3D analysis. The dotted line crossing the upper narrow strip represents the result of the AdS/QCD model [28], while the analogous result of the DSE approach [29] is marked by the solid (blue) line just above the upper narrow strip. Note our further explanations in the text.

for detailed comparisons we refer to [7, 8]. We show in the left panel of Fig. 2 the profiles of the pion DAs in our scheme and two other approaches. The (green) shaded band between the broken lines contains the BMS-like DAs from [20], with the BMS model DA being denoted by a solid line, evolved to the scale 2 GeV. The two broad DAs show the profiles of, respectively, an AdS/QCD model [28], (reviewed in [35]) — dotted curve — and the DA obtained within the Dyson-Schwinger-equation (DSE) based approach of [29, 36] — (blue) solid curve. The dashed-dotted line shows the asymptotic DA. In the right panel of Fig. 2, we show our predictions for $Q^2F_{\gamma^*\gamma^*\pi^0}(Q^2)$ in the form of a (green) shaded band that contains the results of the 2D analysis, including the main theoretical uncertainties. The additional uncertainties, induced by the inclusion of the coefficient a_6, are displayed in the form of (blue) strips above and below the wider band. For comparison, we also show the results for this observable obtained from the most recent dynamical chiral-symmetry preserving Dyson-Schwinger kernels currently available [29] (blue solid line just above the band of our predictions). The result of the AdS/QCD model of [28] is displayed by a dotted line grossly coinciding with our predictions. In order to take into account the evolution with Q^2, we applied the

following procedure: (i) We expanded the corresponding DAs in terms of Gegenbauer harmonics keeping only the first 6 terms. We justified this approximate treatment by computing the errors of truncation. We found that up to 40 GeV^2 the contributions from the last considered term (a_{12}) are of the order of about 0.5% for both models AdS/QCD DA [28] and DSE DA [29]. These values confirm the saturation of the truncated Gegenbauer expansion. (ii) We evolved the expanded DAs from their proprietary scales (1 GeV for the AdS/QCD DA [28] and 2 GeV for the DSE DA [29]) to the factorization scale which we set equal to the large photon virtuality, i.e., $\mu_{\rm F}^2 = Q^2$. (iii) We calculated the scaled form factors shown on the right panel of Fig. 2 by means of the sum rule given by Eq. (2). We emphasize that the predictions for these two external DA models have been calculated in an approximate way serving mainly for illustration. Including a larger number of Gegenbauer harmonics into the expansion of these DAs would eventually provide a still better agreement with the asymptotic limit at high Q^2. Nevertheless, as one observes, both curves agree rather well with the extended band of our predictions and asymptotic QCD, though the underlying pion DAs have very different profiles at low-momentum scales — Fig. 2, left panel. It is worth mentioning that our predictions show a similar good agreement with those obtained in [37, 38] within a QCD-inspired light-front quark approach.

IV. CONCLUSIONS

We have discussed in this paper the theoretical calculation of two-photon exclusive processes $\gamma^* + \gamma \to M$ ($M = \pi^0, \eta, \eta'$) using light-cone sum rules with perturbative input at the NLO, combined with (nonperturbative) pion distribution amplitudes obtained from QCD sum rules with nonlocal condensates. We found that our predictions, which include various theoretical uncertainties of the QCD approach, conform with most available experimental data measured by different Collaborations (CELLO, CLEO, BaBar, and Belle), apart from the high-Q^2 data for the pion-photon transition form factor of the BaBar experiment that violate QCD scaling above ~ 10 GeV^2. These predictions do not employ any fit parameters nor do they need adjustment of the original parameters a_2 and a_4, derived in [20] to the considered data sets. The observed agreement improves further, if we include into the Gegenbauer expansion of the pion distribution amplitude the third coefficient a_6, promoting the original Bakulev-Mikhailov-Stefanis approach [20] to a 3D analysis [9]. Remarkably, our predictions have large overlap with those derived from holographic AdS/QCD [28] and the most recent DCS-improved kernel in a DS-based approach [29]. Our results support the conclusion [9] that the distribution amplitudes of the pion and the nonstrange component of

η and η', i.e., $|n\rangle = (1/\sqrt{2})(|u\bar{u}\rangle + |d\bar{d}\rangle)$, have similar shapes with no indication for a significant $SU(3)_{\rm F}$ flavor asymmetry. In fact, our predictions for the scaled transition form factors for both mesons, π^0 and $|n\rangle$, are in good agreement with the scaling behavior at high Q^2, derived from the collinear factorization properties of QCD.

Acknowledgments

Work partly supported by the Heisenberg-Landau Program 2013 and the Russian Foundation for Fundamental Research (Grants No. 12-02-00613a and 11-01-00182a). A.V.P. acknowledges support by HadronPhysics2, Spanish Ministerio de Economia y Competitividad and EU FEDER under Contracts FPA2010-21750-C02-01, AIC10-D-000598, and GVPrometeo2009/129.

---

[1] Lepage, G.P., Brodsky, S.J.: Exclusive processes in perturbative quantum chromodynamics. Phys. Rev. D **22**, 2157 (1980)

[2] Brodsky, S.J., Lepage, G.P.: Large Angle Two Photon Exclusive Channels in Quantum Chromodynamics. Phys. Rev. D **24**, 1808 (1981)

[3] Efremov, A.V., Radyushkin, A.V.: Asymptotical behavior of pion electromagnetic form factor in QCD. Theor. Math. Phys. **42**, 97 (1980)

[4] Bakulev, A.P., Mikhailov, S.V., Stefanis, N.G.: Unbiased analysis of CLEO data beyond LO and pion distribution amplitude. Phys. Rev. D **67**, 074012 (2003)

[5] Bakulev, A.P., Mikhailov, S.V., Stefanis, N.G.: CLEO and E791 data: A smoking gun for the pion distribution amplitude? Phys. Lett. B **578**, 91 (2004)

[6] Bakulev, A.P., Mikhailov, S.V., Stefanis, N.G.: Tagging the pion quark structure in QCD. Phys. Rev. D **73**, 056002 (2006)

[7] Bakulev, A.P., Mikhailov, S.V., Pimikov, A.V., Stefanis, N.G.: Pion-photon transition—the new QCD frontier. Phys. Rev. D **84**, 034014 (2011)

[8] Bakulev, A.P., Mikhailov, S.V., Pimikov, A.V., Stefanis, N.G.: Comparing antithetic trends of data for the pion-photon transition form factor. Phys. Rev. D **86**, 031501 (2012)

[9] Stefanis, N.G., Bakulev, A.P., Mikhailov, S.V., Pimikov, A.V.: Can We Understand an Auxetic Pion-Photon Transition Form Factor within QCD? Phys. Rev. D **87**, 094025 (2013)

[10] Khodjamirian, A.: Form factors of $\gamma^*\rho \to \pi$ and $\gamma^*\gamma \to \pi^0$ transitions and light-cone sum rules. Eur. Phys. J. C **6**, 477 (1999)

[11] Schmedding, A., Yakovlev, O.: Perturbative effects in the form factor $\gamma\gamma^* \to \pi^0$ and extraction of the pion wave function from CLEO data. Phys. Rev. D **62**, 116002 (2000)

[12] Balitsky, I.I., Braun, V.M., Kolesnichenko, A.V.: Radiative Decay Sigma$^+$ $\to$ p gamma in Quantum Chromodynamics. Nucl. Phys. B **312**, 509 (1989)

[13] Behrend, H.J., et al: A measurement of the π^0, η and η' electromagnetic form-factors. Z. Phys. C **49**, 401 (1991)

[14] Gronberg, J., et al: Measurements of the meson photon transition form factors of light pseudoscalar mesons at large momentum transfer. Phys. Rev. D **57**, 33 (1998)

[15] Aubert, B., et al: Measurement of the $\gamma\gamma^* \to \pi^0$ transition form factor. Phys. Rev. D **80**, 052002 (2009)

[16] Uehara, S., et al: Measurement of $\gamma\gamma^* \to \pi^0$ transition form factor at Belle. Phys. Rev. D **86**, 092007 (2012)

[17] del Amo Sanchez, P., et al: Measurement of the $\gamma\gamma^* \to \eta$ and $\gamma\gamma^* \to \eta'$ transition form factors. Phys. Rev. D **84**, 052001 (2011)

[18] Mikhailov, S.V., Stefanis, N.G.: Transition form factors of the pion in light-cone QCD sum rules with next-to-next-to-leading order contributions. Nucl. Phys. B **821**, 291 (2009)

[19] Efremov, A.V., Radyushkin, A.V.: Factorization and asymptotic behaviour of pion form factor in QCD. Phys. Lett. B **94**, 245 (1980)

[20] Bakulev, A.P., Mikhailov, S.V., Stefanis, N.G.: QCD-based pion distribution amplitudes confronting experimental data. Phys. Lett. B **508**, 279 (2001)

[21] Mikhailov, S.V., Radyushkin, A.V.: Nonlocal condensates and QCD sum rules for pion wave function. JETP Lett. **43**, 712 (1986)

[22] Mikhailov, S.V., Radyushkin, A.V.: Quark condensate nonlocality and pion wave function in QCD. Sov. J. Nucl. Phys. **49**, 494 (1989)

[23] Mikhailov, S.V., Radyushkin, A.V.: The pion wave function and QCD sum rules with nonlocal condensates. Phys. Rev. D **45**, 1754 (1992)

[24] Stefanis, N.G., Schroers, W., Kim, H.C.: Pion form factors with improved infrared factorization. Phys. Lett. B **449**, 299 (1999)

[25] Stefanis, N.G., Schroers, W., Kim, H.C.: Analytic coupling and Sudakov effects in exclusive processes: Pion and $\gamma^*\gamma \to \pi^0$ form factors. Eur. Phys. J. C **18**, 137 (2000)

[26] Agaev, S.S., Braun, V.M., Offen, N., Porkert, F.A.: Light cone sum rules for the $\pi^0\gamma^*\gamma$ form factor revisited. Phys. Rev. D **83**, 054020 (2011)

[27] Agaev, S., Braun, V., Offen, N., Porkert, F.: BELLE Data on the $\pi^0\gamma^*\gamma$ Form Factor: A Game Changer? Phys. Rev. D **86**, 077504 (2012)

[28] Brodsky, S.J., Cao, F.G., de Teramond, G.F.: Evolved QCD predictions for the meson-photon transition form factors. Phys. Rev. D **84**, 033001 (2011)

[29] Chang, L., Cloet, I., Cobos-Martinez, J., Roberts, C., Schmidt, S., et al: Imaging dynamical chiral symmetry breaking: pion wave function on the light front. Phys. Rev. Lett. **110**, 132001 (2013)

[30] Kochelev, N., Vento, V.: Gluonic components of the pion and the transition form factor $\gamma^*\gamma^* \to \pi^0$. Phys. Rev. D **81**, 034009 (2010)

[31] Noguera, S., Vento, V.: Model analysis of the world data on the pion transition form factor. Eur. Phys. J. A **48**, 143 (2012)

[32] Dorokhov, A., Kuraev, E.: Pion transition form factor in the constituent quark model. Phys. Rev. D **88**, 014038 (2013)

[33] Kroll, P.: The form factors for the photon to pseudoscalar meson transitions - an update. Eur. Phys. J. C **71**, 1623 (2011)

[34] Li, H.N., Shen, Y.L., Wang, Y.M.: Joint resummation for pion wave function and pion transition form factor. JHEP **1401**, 004 (2014)

[35] Brodsky, S.J., de Teramond, G.F., Dosch, H.G.: QCD on the Light-Front – A Systematic Approach to Hadron Physics. (2013)

[36] Cloet, I.C., Roberts, C.D.: Explanation and Prediction of Observables using Continuum Strong QCD. arXiv:1310.2651

[37] El-Bennich, B., de Melo, J., Frederico, T.: A combined study of the pion's static properties and form factors. Few Body Syst. **54**, 1851 (2013)

[38] de Melo, J., El-Bennich, B., Frederico, T.: The photon-pion transition form factor: incompatible data or incompatible models? arXiv:1312.6133